

Stimulated emission from multilayer graphene

Ken-ichi Sasaki*

*NTT Research Center for Theoretical Quantum Physics and NTT Basic Research Laboratories,
NTT Corporation, 3-1 Morinosato Wakamiya, Atsugi, Kanagawa 243-0198, Japan*

Kenichi Hitachi

*NTT Basic Research Laboratories, NTT Corporation,
3-1 Morinosato Wakamiya, Atsugi, Kanagawa 243-0198, Japan*

Masahiro Kamada, Takamoto Yokosawa, Taisuke Ochi, and Tomohiro Matsui†

*Advanced Research Laboratory, Anritsu Corporation,
5-1-1 Onna, Atsugi, Kanagawa 243-8555, Japan*

(Dated: August 3, 2022)

Monolayer graphene absorbs ~ 2.3 percent of the incident visible light. This “small” absorption was used to emphasize visual transparency of graphene, but in fact it means that multilayer graphene absorbs sizable fraction of incident light, which causes non-negligible fluorescence. In this paper, we study the light emission properties of multilayer graphene composed of tens to hundreds of layers, because these are informative materials having interesting optical properties correlated closely with fluorescence. For example, it was recently predicted that 87-layer graphene absorbs infrared light at maximum efficiency and 20-layer graphene on silicon substrates exhibits zero reflectance (a total absence of backscattering) at a specific visible light wavelength. By modeling light emissions from multilayer graphene using a transfer matrix method, we could quantitatively explain the measured reflectivity from multilayer graphene on silicon substrates. We found sizable corrections, that cannot be classified as incoherent light emissions, to the reflectance of visible light. The new component originates from stimulated emission caused by absorption at each graphene layer, and it is a coherent sum over the amplitudes coming from all graphene layers with a common phase shift of π relative to the incident light. The coherent corrections to the reflectance become dominant for samples thicker than 40-layers and thinner than 160-layers. Multilayer graphene thus functions as a partial coherent light source of various wavelengths and it may have surface-emitting laser applications.

I. INTRODUCTION

Visual detection of graphene on Si substrates is a common task, but has the aspect of being a nontrivial scientific problem.^{1–3} The difference between the reflectance from the substrate and from graphene on the substrate has to be sufficiently large to increase their contrast, and it is known that Si substrates with a certain thickness of SiO₂ (d_{SiO_2}) have some advantage in this regard.⁴ Namely, when the optical distance of the SiO₂ layer is one-half (or three-halves) the light wavelength used, not only are the two reflectances minimized by destructive interference but their difference (contrast) reaches a maximum. The physics behind this increase in the visibility of graphene is useful not just for searching for graphene but also for exploring notable phenomena. For example, we show that the reflectance of 20 layers of graphene on Si substrate can become zero for normally incident visible light with a wavelength $\lambda \simeq 2d_{\text{SiO}_2}$. Zero reflectance is achieved with the destructive interference caused by SiO₂ and additional interference from multilayer graphene. The interference of light is significant when there is a path difference on the order of a wavelength, but it may be sizable even when the path difference is much shorter than a wavelength (the thickness of 20-layer graphene is only ~ 6 nm). Such a peculiar situation can be realized in a system with a large absorption

coefficient, like graphene.^{5–7} In addition, the reflectance of such system is determined complexly because a large absorption may produce non-negligible luminescence.^{8,9}

In this paper, we define, using a transfer-matrix method, coherent and incoherent corrections to the reflectance of multilayer graphene on Si substrates that are caused by photon emission after the graphene absorbs the incident light. By comparing the calculated and measured reflectivities for various layer numbers, we identified the dependence of the coherent and incoherent components on the number of layers N . We found that even though the branching ratio of the coherent light to the incoherent light is only one percent, the coherent components dominate the incoherent ones for N above approximately 40. Meanwhile, we found that phase fluctuations cause the coherence to become suppressed when N is above approximately 160. The origin of the coherent components is the emission of coherent photons that is stimulated by the scattered light in view of the phase given by π , while the incoherent ones are related to Raman scattering.

This paper is organized as follows. In Sec. II, we review the reflectance without light emission, which provides a starting point of this study. The theory includes only the light scattering and absorption caused by dynamical conductivity of each graphene layer and the substrate. We pay a special attention to the result that the reflectance of 20 layers of graphene on Si substrate can

become zero for normally incident visible light with a wavelength $\lambda \simeq 2d_{\text{SiO}_2}$, because the system is most useful in exploring the corrections to the reflectance. In Sec. III, we examine the corrections to the reflectance due to light emissions. The contributions of light emissions to the reflectance are divided into two categories in terms of the coherence, where coherent emission corresponds to stimulated emission with a common phase, while incoherent emission with a random phase is identified as Raman scattering. The comparison between calculated and measured reflectivities is shown in Sec. IV. Our discussion and conclusion are provided in Sec. V.

II. REFLECTANCE WITHOUT LIGHT EMISSION

Because of the conical energy-band structure of graphene known as the Dirac cone, the dynamical conductivity is well approximated by $\pi\alpha$ for visible light,¹⁰

where α is the fine-structure constant ($\sim 1/137$). As a result, monolayer graphene absorbs ~ 2.3 percent ($= \pi\alpha$) of the incident visible light.¹⁰ A straightforward consequence of this dynamical conductivity, with the understanding that the effect of the stacking order on the reflectance appears in the infrared regime (Sec. V), is that the relative permittivity of graphite is given by

$$\varepsilon_g = \varepsilon_r + i\frac{\alpha\lambda}{2d}, \quad (1)$$

for visible light wavelengths λ ,^{11,12} where d denotes the interlayer spacing (0.335 nm) and ε_r is the dielectric constant of the interlayer space (we assume $\varepsilon_r = 4$ [see Appendix A]).¹³ Although α is certainly a small quantity, since visible light has a much longer λ (400~800 nm) than d , the imaginary part of ε_g is above the real part ε_r .

For the system shown in Fig. 1(a), the reflectance to normally incident light of wavelength λ coming from air is formulated as¹⁴

$$R_N(\lambda) = |c_N^r(\lambda)|^2 = \left| \frac{\left[(n_{\text{Si}} - 1) \cos \varphi + i \left(\frac{n_{\text{Si}}}{n_{\text{SiO}_2}} - n_{\text{SiO}_2} \right) \sin \varphi \right] \cos \phi + \left[\left(\frac{n_{\text{SiO}_2}}{\sqrt{\varepsilon_g}} - \frac{n_{\text{Si}}\sqrt{\varepsilon_g}}{n_{\text{SiO}_2}} \right) \sin \varphi + i \left(\frac{n_{\text{Si}}}{\sqrt{\varepsilon_g}} - \sqrt{\varepsilon_g} \right) \cos \varphi \right] \sin \phi}{\left[(n_{\text{Si}} + 1) \cos \varphi - i \left(\frac{n_{\text{Si}}}{n_{\text{SiO}_2}} + n_{\text{SiO}_2} \right) \sin \varphi \right] \cos \phi - \left[\left(\frac{n_{\text{SiO}_2}}{\sqrt{\varepsilon_g}} + \frac{n_{\text{Si}}\sqrt{\varepsilon_g}}{n_{\text{SiO}_2}} \right) \sin \varphi + i \left(\frac{n_{\text{Si}}}{\sqrt{\varepsilon_g}} + \sqrt{\varepsilon_g} \right) \cos \varphi \right] \sin \phi} \right|^2, \quad (2)$$

where n_{Si} and n_{SiO_2} are the refractive indexes of Si and SiO₂, respectively. Si is treated as an absorbing substrate (n_{Si} is a complex number) whose λ dependence is taken into account,¹⁵ while SiO₂ is treated as an absorption-free film with a λ -independent n_{SiO_2} . The $R_N(\lambda)$ value depends sensitively on the two phases, φ and ϕ ; $\varphi \equiv n_{\text{SiO}_2} \frac{2\pi}{\lambda} d_{\text{SiO}_2}$ is the phase acquired by light after it propagates through a distance d_{SiO_2} in SiO₂ and $\phi \equiv \sqrt{\varepsilon_g} \frac{2\pi}{\lambda} d_N$ is the complex phase acquired when light passes through N -layer graphene of thickness $d_N = Nd$. When $N = 0$ or $\phi = 0$ in Eq. (2), $R_0(\lambda)$ corresponds to the reflectance of the substrate without graphene. It can be minimized for specific λ by destructive interference; namely, $R_0(\lambda)$ is at a minimum when $\cos \varphi = 0$ as $\left| \frac{n_{\text{Si}} - n_{\text{SiO}_2}^2}{n_{\text{Si}} + n_{\text{SiO}_2}^2} \right|^2$.¹⁴ Monolayer graphene is most easily detectable on Si substrates when destructive interference occurs, because $|R_0(\lambda) - R_1(\lambda)|$ takes a maximum when $\cos \varphi = 0$.⁴

The complex phase ϕ causes a further suppression of the reflectance beyond that of φ . Intriguingly, when destructive interference takes place ($\varphi = 3\pi/2$), $R_N(\lambda)$ vanishes for $N \simeq 20$ and $\lambda \simeq 2d_{\text{SiO}_2}$ [see Fig. 1(b) and (c)], which has been referred to as zero reflection.¹⁴ The contrast, defined as $1 - \frac{R_N(\lambda)}{R_0(\lambda)}$, indicates that 20-layer graphene is most easily detectable on the substrate be-

cause the maximum contrast (unity) is at 20 layers, even though it does not reflect light. To capture the essential role of graphene in achieving zero reflection, let us consider a large n_{Si} value in Eq. (2) when $\cos(\varphi) = 0$. For the numerator to vanish, $i \cos \phi - \sqrt{\varepsilon_g} \sin \phi = 0$ has to be satisfied. Since ϕ is small, this equation can be simplified as $i - \varepsilon_g \frac{2\pi d_N}{\lambda} \sim i - i\alpha\pi N$, which shows that $N \sim \frac{1}{\pi\alpha}$ is an approximate layer number that gives zero reflection. Of course, this argument is crude (we have not used the actual values of ε_r , n_{Si} and n_{SiO_2}) as $1/\pi\alpha$ is almost double the exact value of 20. However, the simplification makes it easy to understand that the dominant imaginary part of ε_g ($\simeq i\alpha\lambda/2d$) is essential to the existence of a zero reflection.

III. CORRECTIONS TO REFLECTANCE BY LIGHT EMISSION

The corrections to the reflectance are the main subjects of this paper.^{8,9} Specifically, we consider the corrections where some fraction of the energy absorbed by the j th layer is transferred to light emitted from that layer [see Fig. 2(a)]. The amplitude of emitted light is assumed to be the square root of the layer absorption,¹² A_j^N , multiplied by the branching ratio, \mathcal{B} , i.e., $\sqrt{(\mathcal{B}/2) A_j^N}$, where

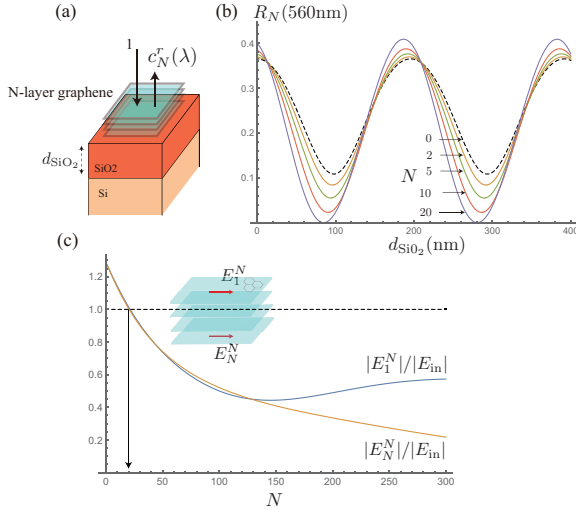


FIG. 1. **Basic optical properties of N -layer graphene on Si substrate.** (a) Schematic diagram of N -layer graphene on top of the substrate, where the Si layer has a semi-infinite thickness. The case of $N = 0$ of $R_N(\lambda) \equiv |c_N^r(\lambda)|^2$, $R_0(\lambda)$, means the reflectance of the substrate without graphene. (b) $R_N(560\text{nm})$ as a function of d_{SiO_2} for different values of N , where $n_{\text{SiO}_2} = 1.43$. Light of $\lambda = 560$ nm is not reflected when $N = 20$ at $d_{\text{SiO}_2} = 280$ nm. (c) Electric field strength of top and bottom layers of N -layer graphene on substrate with $d_{\text{SiO}_2} = 280$ nm. The dashed line, $|E_j^N|/|E_{in}| = 1$, shows the special zero-reflection feature that the scattered component is all absorbed by 20-layer graphene.

$1/\sqrt{2}$ means that light emission is direction-independent along the c -axis. Note that A_j^N depends not only on j and N values but also on d_{SiO_2} and λ .¹⁶

To examine the effect of light emission from the j th layer on the reflectance, we define two subsystems, as shown in Fig. 2(b): one is an isolated $(j - 1)$ -layer graphene in air; the other is $(N - j)$ -layer graphene on the Si substrate. Using the transfer matrix method, we can obtain the transmission and reflection coefficients of an isolated $(j - 1)$ -layer graphene in air [c_{j-1}^{tg} and c_{j-1}^{rg}] and the reflection coefficient of $(N - j)$ -layer graphene on the Si substrate [c_{N-j}^r].^{11,12} Let the reflection coefficients X_j and Y_j , and transmission coefficient Z_j for the combined subsystems [see Fig. 2(b)]. These can be obtained by a self-consistent method as follows. After calculating $X_j^{(n)}$, we add it

to $\sqrt{(\mathcal{B}/2) A_j^N}$ of the incident light to the $(j - 1)$ -layer graphene (in air) as $\sqrt{(\mathcal{B}/2) A_j^N} + X_j^{(n)}$ and recalculate $Y_j^{(n+1)} = c_{j-1}^{rg} \left(\sqrt{(\mathcal{B}/2) A_j^N} + X_j^{(n)} \right)$ and $Z_j^{(n+1)} = c_{j-1}^{tg} \left(\sqrt{(\mathcal{B}/2) A_j^N} + X_j^{(n)} \right)$. Then, we add a new $Y_j^{(n+1)}$ to $\sqrt{(\mathcal{B}/2) A_j^N}$ of the incident light to the $(N - j)$ -layer graphene on the Si substrate as $\sqrt{(\mathcal{B}/2) A_j^N} + Y_j^{(n+1)}$ and recalculate $X_j^{(n+1)} = c_{N-j}^r \left(\sqrt{(\mathcal{B}/2) A_j^N} + Y_j^{(n+1)} \right)$. These computations are repeated until X_j and Y_j converge. In this way, we can obtain an analytical expression of the converged Z_j for a given \mathcal{B} as

$$Z_j(\mathcal{B}) = c_{j-1}^{tg} \left\{ \frac{1 + c_{N-j}^r}{1 - c_{N-j}^r c_{j-1}^{rg}} \right\} \sqrt{\left(\frac{\mathcal{B}}{2}\right) A_j^N}. \quad (3)$$

The electric field at an infinitesimal distance above and below the j th layer becomes $\sqrt{(\mathcal{B}/2) A_j^N} + X_j^{(n)} + Y_j^{(n+1)}$ and $\sqrt{(\mathcal{B}/2) A_j^N} + Y_j^{(n)} + X_j^{(n+1)}$, respectively. Self-consistency is therefore essential to ensure that the electric field component is continuous at the j th layer, which is a requirement of the Maxwell equations.

$Z_j(\mathcal{B})$ is the value at zero initial phase, so the transmission coefficient can be given a phase degree of freedom expressing the timing of photon emissions from the different layers:

$$z^N \equiv \sum_{j=1}^N e^{i\theta_j} Z_j(\mathcal{B}). \quad (4)$$

Accordingly, the corrected reflectance is uniquely determined by $R_N \equiv |c_r^N + z^N|^2 = |c_r^N|^2 + 2\text{Re}[c_r^N z^N] + |z^N|^2$. The change in the reflectance due to the corrections depends on these phases θ_j .¹⁷ In the case that θ_j is a random variable, the time average leads to an incoherent summation because $\langle |z^N|^2 \rangle \rightarrow \sum_{j=1}^N |Z_j(\mathcal{B})|^2$ and $\langle \text{Re}[c_r^N z^N] \rangle \rightarrow 0$.¹⁸ In the case that θ_j has the average expectation value θ , which is uniform over different j and the fluctuation in θ_j at each j is suppressed, the reflectance leads to $R_N = \left| c_r^N + e^{i\theta} \sum_{j=1}^N Z_j(\mathcal{B}) \right|^2$. In principle, θ may depend on N and λ as $\theta(N, \lambda)$, but for a start we will simply treat it as a constant parameter. Here, we can define a generalized reflection formula covering these two cases as

$$R_N(\lambda, \theta, \mathcal{B}_{coh}, \mathcal{B}_{inc}) \equiv \left| c_r^N + e^{i\theta} \sum_{j=1}^N Z_j(\mathcal{B}_{coh}) \right|^2 + \sum_{j=1}^N |Z_j(\mathcal{B}_{inc})|^2, \quad (5)$$

where \mathcal{B}_{inc} is the branching ratio of incoherent photon emissions, in which light emitted from each layer contributes independently to the reflectance. Since $Z_j(\mathcal{B})$ are proportional to $\sqrt{\mathcal{B}}$ [Eq. (3)], the incoherent corrections [last term of Eq. (5)] are proportional to \mathcal{B}_{inc} . In contrast, \mathcal{B}_{coh} is the branching ratio of coherent emissions, whose amplitude should be added to the reflection coefficient c_r^N . As a result, though $\sum_{j=1}^N Z_j(\mathcal{B}_{coh})$ is a complex number proportional to $\sqrt{\mathcal{B}_{coh}}$, coherent corrections can increase or decrease the reflectance depending on the coherent phase θ .

Incoherent photons are emitted by inelastic scattering of light, such as Raman scattering. Namely, the reflectance of a specific light frequency (ω) undergoes the incoherent corrections especially when a white-light beam is used as an excitation source, since it contains various frequencies ω_e above ω , where $\omega_e - \omega$ corresponds to the frequency of the Raman active phonon modes. For Raman scattering, the parameter \mathcal{B}_{inc} is fundamentally determined by the electron-photon and electron-phonon coupling strengths, and should not be so sensitive to the change in N . Indeed, the incoherent corrections with a constant \mathcal{B}_{inc} follow roughly measured N -dependence of the G-band Raman intensity [Appendix B]. Note that the incoherent corrections always increase the reflectance and preclude zero reflections. Moreover, the G-band Raman intensity is enhanced when zero reflection occurs,^{9,19–21} which is known as interference-enhanced Raman scattering.⁸ Meanwhile, coherent photon emission originates from the annihilation of photo-excited electron-hole pairs by the electron-photon coupling strength, and like \mathcal{B}_{inc} , \mathcal{B}_{coh} should be insensitive to changes in N . When $\mathcal{B}_{coh} = \mathcal{B}_{inc} = 0$, $R_N(\lambda, \theta, \mathcal{B}_{coh}, \mathcal{B}_{inc})$ reduces to Eq. (2). All calculations presented in this paper assume that $\mathcal{B}_{inc} = 0.1$ and $\mathcal{B}_{coh} = 0.001$ [see Fig. 2(c)].

IV. COMPARISON BETWEEN CALCULATED AND MEASURED REFLECTANCE

Multilayer graphene was prepared by exfoliating highly oriented pyrolytic graphite (HOPG) on SiO₂/Si substrate, and the thickness of the graphene flake was determined by atomic force microscopy (Dimension XR, Bruker). The reflectance of the multilayer graphene was measured with a spectroscopic reflectometer (TohoSpec3100, Toho Technology) using an objective lens of $\times 50$. The reflectometer was also used to determine the thickness of the SiO₂ substrate (274 ± 1 nm).

We calculated Eqs. (2) and (5) for graphene with $N = 0, 1, 4, 7, 24, 26, 28, 37, 38, 40, 47, 54, 55, 60, 64, 70, 97, 108, 110, 122, 135, 160, 226,$ and 319 layers on the same Si substrate and compared the calculated results with measured reflectivities. Representative measured and calculated spectral reflectivities are presented in Figs. 3 and 4.

First, we determined that $n_{\text{SiO}_2} = 1.43$ (and $d_{\text{SiO}_2} = 274$ nm) from the reflectance of the substrate shown in

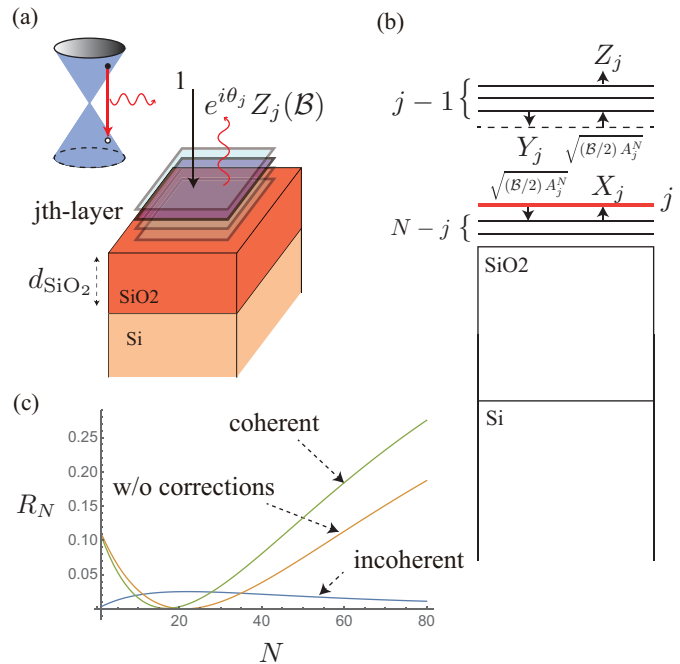


FIG. 2. **Light emission from N -layer graphene on Si substrate.** (a) Corrections to the reflectivity arise because some fraction of the electron-hole pairs created by the photon absorption emit light (luminescence). The corrections to the reflectivity of each layer are summed using Eq. (4). (b) Z_j is calculated self-consistently as explained in the text. (c) Dependence of the corrections to $R_N(560\text{nm})$ on N , where $d_{\text{SiO}_2} = 280$ nm, $\mathcal{B}_{inc} = 0.1$, $\mathcal{B}_{coh} = 0.001$ and $\theta = \pi$. The incoherent components are enhanced (which is known as interference-enhanced Raman scattering) at around 20 layers. The coherent components can make positive and negative contributions to the reflectance, without spoiling the zero reflection property while the layer number is shifted.

the upper left panel in Fig. 3. These values are used consistently in all the calculations reported in this paper. The two curves overlap from 460 to 560 nm, while Eq. (2) underestimates the reflectance for $\lambda < 460$ nm and $\lambda > 560$ nm. The origin of the discrepancy between the measured and calculated values is unclear.

When N is small, e.g., 7, there are incoherent corrections around the minimum reflectance. However, the incoherent corrections are almost canceled by the coherent ones. As a result, Eq. (2) happens to coincide to the measured reflectance.

Next, we focused on the reflectance of 24-layer graphene, which is closest in layer number to the invisible 20-layer graphene. The incoherent corrections are significant, which is expected as the interference-enhanced Raman scattering. Meanwhile, the coherent component improves the fitting. For all the samples with fewer than 122 layers, the coherent corrections to the reflectance are essential to improving the fitting because the incoherent corrections decrease with increasing N and the coherent

corrections dominate the incoherent ones above $N = 40$. For all the samples fewer than 122 layers (except 26 and 28-layer [Appendix B]), we conclude that $\theta = \pi$ is the reasonable choice to explain the measurements.

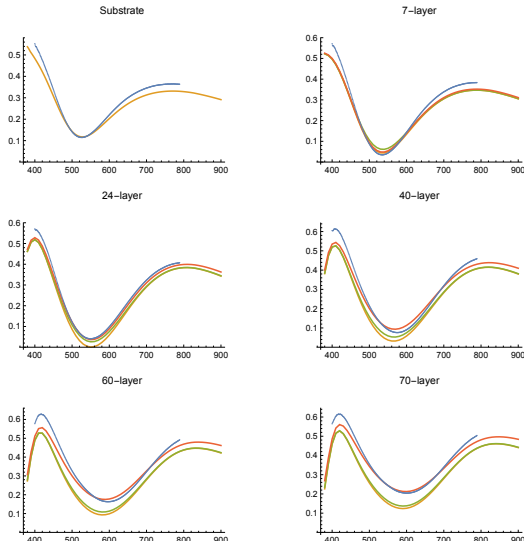


FIG. 3. Measured (blue) and calculated (yellow, green and red) spectral reflectivities of N -layer graphene on the same Si substrate. A white-light source was used, and the reflectivity was measured at room temperature. The yellow curves are for Eq. (2), which does not include corrections. The green ones include only incoherent corrections. The red curves include both incoherent and coherent corrections. The horizontal axis is λ (nm), and the reliable range of our spectrometer is 450 to 800 nm.

In the case of 160 layers, we noticed a difference between the two curves (red and blue). This can be attributed to either that the value of \mathcal{B}_{coh} is suppressed or θ starts to deviate from π . The later is more plausible because the coherent corrections are necessary to explain the reflectance of graphite [Appendix C].

In the case of 226 layers, the inclusion of the coherent correction with $\theta = \pi$ results in a large discrepancy in the spectrum. This suggests two possibilities for θ . One is that θ actually depends on N and λ . The right panel is plotted using $\theta = 3\pi/4$. Although the fitting is improved by this small shift in θ from π , there is a frequency region ($\lambda < 500$ nm) where the change in θ increases the discrepancy. The other, more plausible, explanation is that θ_j starts to fluctuate between π and 0 at every layer. As a result, θ deviates from π and coherence is partially lost. In the case of 319 layers, the left panel in Fig. 4 shows that $\theta = \pi$ seems appropriate for $\lambda < 500$ nm, while the right panel shows that $\theta = 3\pi/4$ improves the fitting for $\lambda > 550$ nm.

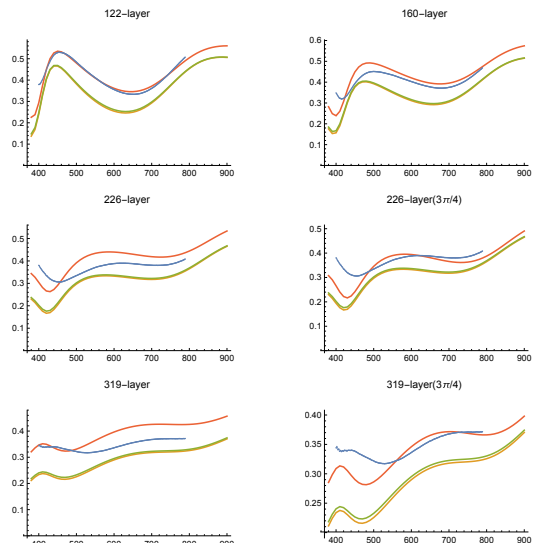


FIG. 4. Measured (blue) and calculated (yellow, green and red) spectral reflectivities of N -layer graphene [large N values]. The graphene samples are thick, so incoherent corrections to the reflectivity are suppressed (the yellow and green curves mostly overlap). For 226- and 319-layer graphene, the coherent corrections in the left (right) panel are calculated with $\theta = \pi$ ($3\pi/4$). The large discrepancy between the blue and red curves suggests either the fluctuation of θ_j is not negligibly small for such thick samples or θ is actually dependent on N and λ .

V. DISCUSSION AND CONCLUSION

Since coherent and incoherent emissions are two extreme cases of the phases θ_j in Eq. (4) (perfectly uniform and random), a sharp distinction between the coherent and incoherent emissions is not always possible. Furthermore, the average value θ in Eq. (5) was found to change from π for graphene multilayer thicker than 160-layer, and unfortunately there seems no clue to predict θ value for them in our theoretical framework. We have tried to improve the fitting, for example, by substituting $e^{i\theta_j}$ of Eq. (4) the complex conjugation of the electric field at the j th layer multiplied by -1 . However, the fittings did not hardly improve. The most proper method to calculate the reflectance is to derive a dynamical model controlling θ_j of Eq. (4) from more microscopic level, presumably quantum theory.

For the coherent photon emissions to be stabilized, there must be a mechanism for developing correlations between different layers.^{17,22} We speculate that motions of photoexcited electrons at the nearest-neighbor layers are mutually synchronized with each other through instantaneous Coulomb interaction. Because the photoexcited electrons in each graphene layer are described as the pseudospin flip,^{22,23} the interaction can lead to a spatial order of pseudospins which may be involved in synchronization of the induced emission. To elucidate

the origin of the coherent corrections experimentally, it will be useful to eliminate the incoherent corrections as much as possible. Since the incoherent corrections originate from inelastic scatterings such as Raman scattering, they must be suppressed by inserting a filter in front of a white-light source and by lowering the temperature. We expect that the signal of coherent corrections would appear most clearly as a shift in N of the invisible 20-layer graphene [see Fig. 2(c)].

Finally, let us discuss another correction to Eq. (2), which is caused by an electronic coupling between the

layers that is expected to exist for natural graphite with AB or AA stacking dominance.^{24,25} The corrections to ε_g due to an interlayer electronic interaction are substantial near the telecom wavelengths of infrared light. By defining $m_r = \gamma_1 \cos\left(\frac{r\pi}{N+1}\right)$, where $r (= 1, \dots, N)$ is the wavenumber of the standing wave formed along the c -axis by an interlayer hopping of $\gamma_1 (= 0.4 \text{ eV})$,^{26,27} we found that the relative permittivity of N -layer graphene with AB and AA stacking is expressed as¹²

$$\varepsilon_g^{\text{AB}} = \varepsilon_r + i \frac{\alpha\lambda}{2dN} \sum_{r=1}^N \left\{ \left(1 - \frac{2m_r}{\hbar\omega - 2m_r}\right) \Theta(\hbar\omega - 2(m_r + |m_r|)) + \left(\frac{2m_r}{\hbar\omega}\right)^2 \Theta(\hbar\omega - 2|m_r|) \right\}, \quad (6)$$

$$\varepsilon_g^{\text{AA}} = \varepsilon_r + i \frac{\alpha\lambda}{2dN} \sum_{r=1}^N \left\{ \Theta\left(2m_r + \frac{\hbar\omega}{2}\right) - \Theta\left(2m_r - \frac{\hbar\omega}{2}\right) \right\}, \quad (7)$$

where $\Theta(x)$ denotes the step function satisfying $\Theta(x) = 1$ for $x \geq 0$ and 0 otherwise. Putting these into Eq. (2), we can obtain the reflectance of multilayer graphene with the stacking order. The effect of the stacking orders appears as a peak structure in the reflectance at a light energy of $2\gamma_1$,^{24,28} which corresponds to telecom wavelengths. A well-defined peak structure appears on the scale of hundreds of layers. Thus, the effect of changing N on the stacking order can be explored. Our samples are HOPG, which contains a much higher density of stacking fault than Kish or natural graphite. The characteristic layer number of stacking fault in HOPG was shown to be 40-layer by scanning tunneling spectroscopy measurements.²⁹ Inclusion of the incoherent and coherent corrections into the analysis would be an interesting way to investigate θ value. The assumptions of $\mathcal{B}_{inc} = 0.1$ and $\mathcal{B}_{coh} = 0.001$ that were used in all of our visible-light calculations should be reconsidered for infrared light because the photo-excited carriers move along the c -axis which may hinder synchronization of pseudospins.

To conclude, we succeeded in explaining the measured visible reflectivity of multilayer graphene samples on Si substrate by including coherent and incoherent light emissions caused by some fraction ($\mathcal{B}_{coh} = 0.001$ and $\mathcal{B}_{inc} = 0.1$) of the absorbed photon energy. The coherent corrections are essential for $40 \lesssim N \lesssim 160$ to assure an agreement between theory and experiment, though \mathcal{B}_{coh} is only one percent of the incoherent component ($\mathcal{B}_{coh}/\mathcal{B}_{inc} = 0.01$). A theoretical prediction about the exact dependence of \mathcal{B}_{coh} on $N (> 160)$ and λ is beyond the scope of this paper, however, existing experimental data have not ruled out the possibility that the coherent emissions exist for graphite. This research framework developed for N -layer graphene is applicable to other layered materials and will advance the use of layered materials in applications such as surface-emitting lasers.

ACKNOWLEDGMENTS

K. S thanks Y. Sekine, H. Endo, and Y. Taniyasu for raising helpful questions on this subject. Part of this work was supported by “Nanotechnology Platform Japan” of the Ministry of Education, Culture, Sports, Science and Technology (MEXT), Grant Number JP-MXP09F21UT0045, and the reflectance measurement was conducted in the Takeda Cleanroom with help of Nanofabrication Platform Center of School of Engineering, the University of Tokyo, Japan.

Appendix A: Optical constants

We assume the relative permittivity of multilayer graphene is of the form of Eq. (1), where ε_r corresponds to the dielectric constant of the interlayer space in our transfer matrix formulation. If the electronic current is sufficiently localized at a graphene layer, the interlayer space is a vacuum, and an appropriate choice would be $\varepsilon_r = 1$. But in fact, because the electronic wave function of the π -orbital spreads into the space between graphene layers, light propagating in the space is likely to be subjected to the spread of the wave function.¹² Reference 13 reported the optical constants (refractive index $n = \text{Re}[\sqrt{\varepsilon_g}]$ and absorption coefficient $k = \text{Im}[\sqrt{\varepsilon_g}]$) of CVD graphene on SiO_2/Si substrates. The experimental n and k values are shown as dots in Fig. 5, where the curves are the optical constants plotted using Eq. (1) with $\varepsilon_r = 1$ and 4. We focused $\varepsilon_r = 4$ (effective refractive index of the interlayer space is $n = 2$) in the main text. Our approach based on the Dirac cone approximation does not include a plasmonic excitation at high energy, which may be the reason for the discrepancy in n between theory and experiments.

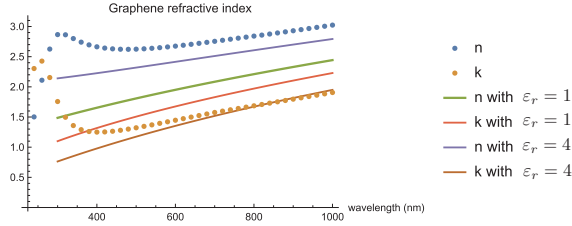


FIG. 5. **Determination of ϵ_r .** Dots are experimental results, taken from Ref. 13, for chemical deposited graphene on SiO₂/Si substrates. A comparison between the measured and calculated reflectivity indicates that $\epsilon_r = 4$ is a reasonable value, though there is still a slight discrepancy between the values of n ($\Delta n \sim 0.2$).

The reflectance takes a minimum at a certain wavelength primarily due to the destructive interference caused by SiO₂. Intriguingly, the position is shifted by the coherent components, as shown in Fig. 6. The shift is fully due to the coherent corrections; the incoherent corrections do not contribute. Moreover, when $\epsilon_r = 1$ is used, an artificial shift in the wavelength is needed to obtain a reasonable fitting. In this sense, the minimum position is informative for determining the value of ϵ_r .

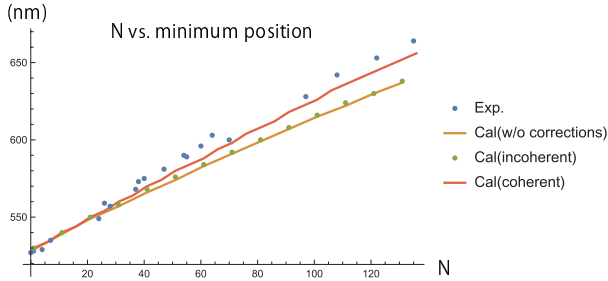


FIG. 6. **N dependence of the wavelength at the minimum reflectance.** Dots are measured wavelengths that give the minimum reflectance. The coherent corrections are essential for avoiding an artificial shift appearing in the reflectance spectrum that may be caused by inappropriate choice of objectives.

Appendix B: Incoherent Raman scattering

To validate the interpretation of the incoherent component as Raman scattering, we measured the G-band Raman peak intensity as a function of N (a light-source with wavelength 532 nm is used). As shown in Fig. 7, there is a reasonable similarity between the measured Raman intensity (dots) and calculated incoherent component [Cal(incoherent) 274 nm], while at small N values below 30, there is a large discrepancy between them.

There are two possible reasons for the discrepancy in small N . First, when $N < 30$, the coherent and incoherent components are of similar magnitude. Thus, there

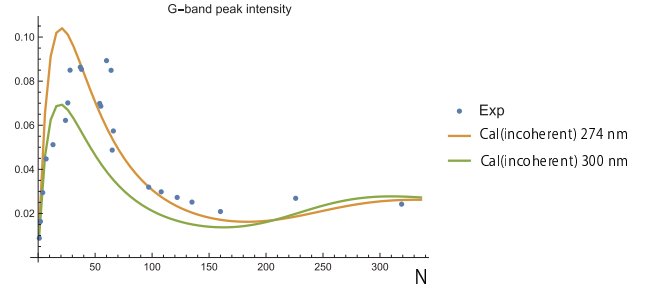


FIG. 7. **Incoherent component characterized as Raman scattering.** Dots are the measured Raman peak intensity of the G-band. Our sample had 274-nm-thick SiO₂; the plot for the 300-nm thickness is to show that the intensity profile is sensitive to the thickness.

might be an intermediate stage where the phase θ_j is neither random nor constant, which invalidates a sharp distinction between them. This argument might explain the anomalous results seen only for the 26- and 28-layer samples, for which $\theta = 0$ gives a better agreement than $\theta = \pi$, as shown in Fig. 8. Second, there is a possibility that the integrated intensity rather than peak intensity should be compared with the incoherent component. Indeed, it is known that the shape of the G-band spectrum is sensitive to the doping level.^{30,31} Furthermore, there are other Raman bands beside the G band, such as 2D band. Perhaps, we need to take into account not only the G band but also the 2D band, as both emit incoherent light.

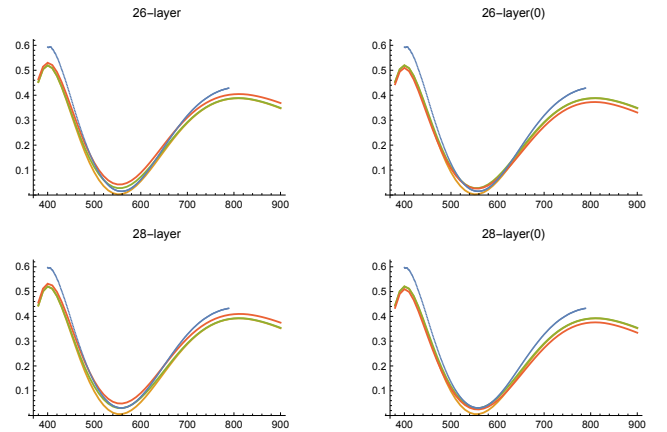


FIG. 8. **Phase θ of coherent component: π and 0.** For only 26- and 28-layer samples, $\theta = \pi$ (left) does not give a reasonable agreement between the calculated and measured reflectance. The phase of $\theta = 0$ (right) improves the fitting. The horizontal axis is λ (nm), and the reliable range of our spectrometer is 450 to 800 nm.

Appendix C: Graphite

The two curves shown in Fig. 9, are the measured and calculated reflectivities of graphite.³² Please note that the theoretical curve does not include the corrections. The fact that they nearly overlap below the photon energy of 0.8 eV suggests that coherent corrections in graphite should disappear for infrared region below 0.8 eV, while the discrepancy between the two curves above 0.8 eV is attributed to coherent corrections. This is possible, for example, when \mathcal{B}_{coh} decreases with increasing N . The critical photon energy of 0.8 eV has a special meaning: the π -electrons can hop between layers below 0.8 eV, because the interlayer hopping integral is $\gamma_1 = 0.4$ eV. Thus, the existence of coherent corrections above 0.8 eV may have some relationship to that (high energy) photoexcited electrons or holes cannot move between different layers.

However, if we are to consider that \mathcal{B}_{coh} does not change from 0.001 and that the phase θ can depend on λ (and N), there is another way of explaining the reflectivity of graphite in terms of coherent corrections. Namely, $|c_r^\infty + e^{i\theta} \sum_{j=1}^{\infty} Z_j(\mathcal{B}_{coh})|^2$ can be equal to $|c_r^\infty|^2$ for a special value of θ . Such a $\theta(\lambda)$ value of graphite is $5\pi/8$ below 0.8 eV and increases very slightly as increasing photon energy. There is an obvious upper bound of $\theta(\lambda)$

as $3\pi/4$. The phase $\theta = \pi$ that was an excellent choice for multilayer graphene below $N = 160$ is no longer valid for graphite.

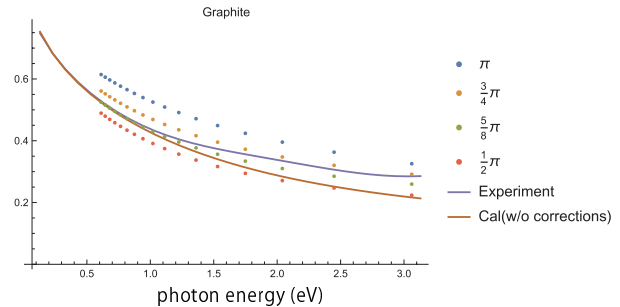


FIG. 9. **Coherent phase of graphite.** The calculated reflectivity (without corrections) reproduces satisfactory the measured reflectivity of graphite for photon energy below 0.8 eV. This does not necessarily mean that coherent corrections are suppressed in graphite. Indeed, coherent corrections are necessary to explain the measured reflectivity of graphite above photon energy 0.8 eV. In these plots, $N = 1500$ which is large enough to simulate graphite.¹¹

-
- * kenichi.sasaki.af@hco.ntt.co.jp
† Tomohiro.Matsui@anritsu.com
- ¹ K. S. Novoselov, A. K. Geim, S. V. Morozov, D. Jiang, M. I. Katsnelson, I. V. Grigorieva, S. V. Dubonos, and A. A. Firsov, *Nature* **438**, 197 (2005).
 - ² Y. Zhang, Y.-W. Tan, H. L. Stormer, and P. Kim, *Nature* **438**, 201 (2005).
 - ³ K. S. Novoselov, D. Jiang, F. Schedin, T. J. Booth, V. V. Khotkevich, S. V. Morozov, and A. K. Geim, *Proceedings of the National Academy of Sciences of the United States of America* **102**, 10414 (2005).
 - ⁴ P. Blake, E. W. Hill, A. H. C. Neto, K. S. Novoselov, D. Jiang, R. Yang, T. J. Booth, and A. K. Geim, *Applied Physics Letters* **91**, 063124 (2007).
 - ⁵ Z. H. Ni, H. M. Wang, J. Kasim, H. M. Fan, T. Yu, Y. H. Wu, Y. P. Feng, and Z. X. Shen, *Nano Letters* **7**, 2758 (2007).
 - ⁶ C. Casiraghi, A. Hartschuh, E. Lidorikis, H. Qian, H. Harutyunyan, T. Gokus, K. S. Novoselov, and A. C. Ferrari, *Nano Letters* **7**, 2711 (2007).
 - ⁷ B. G. Ghamsari, J. Tosado, M. Yamamoto, M. S. Fuhrer, and S. M. Anlage, *Scientific Reports* 2016 6:1 **6**, 1 (2016).
 - ⁸ R. J. Nemanich, C. C. Tsai, and G. A. N. Connell, *Physical Review Letters* **44**, 273 (1980).
 - ⁹ Y. Y. Wang, Z. H. Ni, Z. X. Shen, H. M. Wang, and Y. H. Wu, *Applied Physics Letters* **92**, 043121 (2008).
 - ¹⁰ R. R. Nair, P. Blake, A. N. Grigorenko, K. S. Novoselov, T. J. Booth, T. Stauber, N. M. R. Peres, and A. K. Geim, *Science* **320**, 1308 (2008).
 - ¹¹ K. Sasaki and K. Hitachi, *Communications Physics* **3**, 90 (2020).
 - ¹² K.-i. Sasaki, *Journal of the Physical Society of Japan* **89**, 094706 (2020).
 - ¹³ M. A. El-Sayed, G. A. Ermolaev, K. V. Voronin, R. I. Romanov, G. I. Tselikov, D. I. Yakubovsky, N. V. Doroshina, A. B. Nemtsov, V. R. Solovey, A. A. Voronov, S. M. Novikov, A. A. Vyshnevyy, A. M. Markeev, A. V. Arsenin, and V. S. Volkov, *Nanomaterials* 2021, Vol. 11, Page 1230 **11**, 1230 (2021).
 - ¹⁴ H. Anders, *Thin Films in Optics* (The Focal Press, 1965).
 - ¹⁵ D. E. Aspnes and A. A. Studna, *Physical Review B* **27**, 985 (1983).
 - ¹⁶ S. Saito, *Statistical Mechanics of the Random Walk* (1965).
 - ¹⁷ Y. Kuramoto, *Springer Series in Synergetics*, **19** (1984), 10.1007/978-3-540-10111-1_1.
 - ¹⁸ N. V. Velson, N. V. Velson, H. Zobeiri, X. Wang, and X. Wang, *Optics Express*, Vol. 28, Issue 23, pp. 35272-35283 **28**, 35272 (2020).
 - ¹⁹ D. Yoon, H. Moon, H. Cheong, J. S. Choi, J. A. Choi, and B. H. Park, *Journal of the Korean Physical Society* **55**, 1299 (2009).
 - ²⁰ X. L. Li, X. F. Qiao, W. P. Han, Y. Lu, Q. H. Tan, X. L. Liu, and P. H. Tan, *Nanoscale* **7**, 8135 (2015).
 - ²¹ Y. S. No, H. K. Choi, J. S. Kim, H. Kim, Y. J. Yu, C. G. Choi, and J. S. Choi, *Scientific Reports* 2018 8:1 **8**, 1 (2018).
 - ²² R. H. Dicke, *Physical Review* **93**, 99 (1954).
 - ²³ K.-i. Sasaki, K. Kato, Y. Tokura, K. Oguri, and T. Sogawa, *Physical Review B* **84**, 085458 (2011).
 - ²⁴ E. A. Taft and H. R. Philipp, *Physical Review* **138**, A197 (1965).
 - ²⁵ M. Hanfland, K. Syassen, and R. Sonnenschein, *Physical Review Letters* **105**, 105501 (2010).

- Physical Review B **40**, 1951 (1989).
- ²⁶ H. Min and A. H. MacDonald, Progress of Theoretical Physics Supplement **176**, 227 (2008).
- ²⁷ B. Partoens and F. M. Peeters, Physical Review B **75**, 193402 (2007).
- ²⁸ M. S. Dresselhaus and G. Dresselhaus, Physical Review B **13**, 4635 (1976).
- ²⁹ T. Matsui, H. Kambara, Y. Niimi, K. Tagami, M. Tsukada, and H. Fukuyama, Physical Review Letters **94**, 226403 (2005).
- ³⁰ A. Das, S. Pisana, B. Chakraborty, S. Piscanec, K. Saha, U. V. Waghmare, K. S. Novoselov, H. R. Krishnamurthy, A. K. Geim, A. C. Ferrari, and A. K. Sood, Nature Nanotechnology **3**, 210 (2008).
- ³¹ K.-i. Sasaki, K. Kato, Y. Tokura, S. Suzuki, and T. Sogawa, Physical Review B **86**, 201403 (2012).
- ³² A. B. Djurišić and E. H. Li, Journal of Applied Physics **85**, 7404 (1999).